CZECH TECHNICAL UNIVERSITY IN PRAGUE

FACULTY OF MECHANICAL ENGINEERING

DOCTORAL THESIS STATEMENT

CZECH TECHNICAL UNIVERSITY IN PRAGUE

FACULTY OF MECHANICAL ENGINEERING

DEPARTMENT OF MECHANICS, BIOMECHANICS AND MECHATRONICS

DOCTORAL THESIS STATEMENT

CELL MECHANICS

by

Ing. Katarína Mendová

Doctoral Study Programme: Mechanical Engineering

Study Field: Biomechanics

Supervisor: prof. RNDr. Matej Daniel, Ph.D.

Doctoral thesis statement to obtain the academic title "Ph.D."

Prague 2024

Název anglicky: Cell mechanics

Disertační práce byla vypracována v kombinované formě doktorského studia na Ústavu mechaniky, biomechaniky a mechatroniky Fakulty strojní ČVUT v Praze.

Disertant: Ing. Katarína Mendová
Ústav mechaniky, biomechaniky a mechatroniky, Fakulta strojní ČVUT v Praze
Technická 4, 160 00, Praha 6, Katarina.Mendova@fs.cvut.cz

Školitel: prof. Ing. Matej Daniel, Ph.D.
Ústav mechaniky, biomechaniky a mechatroniky, Fakulta strojní ČVUT v Praze
Technická 4, 160 00, Praha 6, Matej.Daniel@fs.cvut.cz

Oponenti doc. Ing. Tomáš Suchý, Ph.D., Fakulta strojní ČVUT v Praze
prof. Ing. Radovan Hudák, Ph.D., Strojnícka fakulta TUKE v Košiciach
prof. MUDr. Jakub Otáhal, Ph.D., 2. Lekářska fakulta UK v Praze.

Teze byly rozeslány dne: .....

Obhajoba disertace se koná dne ..... v …… hod.

v zasedací místnosti č. 623 (6. patro) Fakulty strojní ČVUT v Praze, Technická 4, Praha 6 před komisí pro obhajobu disertační práce ve studijním oboru Biomechanika.

S disertací je možno se seznámit na oddělení vědy a výzkumu Fakulty strojní ČVUT v Praze, Technická 4, Praha 6.

prof. RNDr. Matej Daniel, Ph.D.

předseda oborové rady oboru Biomechanika

Fakulta strojní ČVUT v Praze

Annotation

As revealed in the literature, there is significant variability in the mechanical properties of living cells. This variability may arise from differences in cell mechanical properties or from variations in experimental setups. To address the latter, we developed a method to manufacture artificial cells to serve as a reference in mechanical testing. In this study, liposomes produced by a microfluidic device were used as standards for testing. To correlate the measured data with the constitutive properties of biomembranes, we developed mathematical models of cell indentation based on a liquid shell description of the biomembrane. Our findings demonstrate that the mechanical properties of liposomes are significantly influenced by the test method and the data processing method used. Additionally, we observed that the commonly used Hertz model underestimates the effect of cell size.

Keywords: Liposomes; microfluidic device; mechanical properties; Young´s modulus; area compressibility modulus

Anotace

Z dostupné literatury o mechanice buněk vyplývá, že živé buňky vykazují různé mechanické vlastnosti. Tato variabilita může být způsobena jak samotnými mechanickými vlastnostmi, tak experimentálním testováním buněk. Pro ověření druhé možnosti jsme vyvinuli metodu výroby umělých buněk, které se pro mechanické testování používají jako referenční. V naší studii sloužily, jako reference pro testování, liposomy vyrobené pomocí mikrofluidního zařízení. Navrhli jsme také matematické modely buněčné indentace s využitím popisu kapalného pláště biomembrány tak, abychom propojili naměřená data s konstitutivními vlastnostmi biomembrány. Výsledky ukázaly, že vlastnosti liposomů jsou značně ovlivněny metodou testování a způsobem zpracování dat. Dále jsme ukázali, že běžně používaný Hertzův model podceňuje vliv velikosti buněk.

Klíčová slova: Liposomy; mikrofluidní zařízení; mechanické vlastnosti; Youngův modul; modul příčné stlačitelnosti

Contents

1 Introduction

All living things are built from fundamental units called cells. These cells perform a variety of essential functions, including providing structure, support, growth, transport, energy production, and reproduction [1]. Biomechanics study of how mechanical forces influence both a cell's form and function, further exploring how cells generate and respond to these physical signals [2]. By studying cellular biomechanics, we gain valuable insights into how cells interact with their surrounding environment, maintain their shape and integrity, sense and adapt to mechanical stimuli, regulate gene expression and differentiation, and ultimately contribute to tissue development and disease processes [1].

The mechanical properties of individual cells are intricately linked to crucial biological processes [3]. Consequently, alterations in these mechanical properties have been associated with various pathological phenomena and diseases [1]. Prior research has established a clear connection between the mechanical characteristics of cells and biological systems within living organisms, with specific examples including adhesion, migration, and cell division [4].

Intriguingly, research suggests that knowledge of a cell's mechanical properties and its response to specific external stimuli could play a role in the early detection of cancer [3]. Recent advancements in experimental techniques have paved the way for measuring the mechanical properties of individual cells and even their subcellular structures. Among these techniques, Atomic Force Microscopy (AFM) is the most widely used to assess cell properties. However, this technique often treats the cell as a linear elastic material characterized by a single modulus of elasticity. This approach presents limitations, as real cells are highly heterogeneous, composed of soft, non-linear materials that are difficult to accurately represent as a simple elastic continuum. Additionally, measurements of the same cell using various methods can yield significantly different results, even with repeated measurements on a single cell. This highlights the need for an engineering approach to cell measurement, one that utilizes standardized protocols while acknowledging the inherent properties of living cells.

The focus of this thesis is twofold: first, we will provide a detailed description of existing experimental methods for measuring cell mechanics. Second, we will introduce novel design, manufacturing, and testing of a novel experimental cell model. This research will involve a comparative analysis of this artificial testing standard's properties across experimental methods and data analysis approaches.

2 State of the art

Cells (Fig. 1) exhibit remarkable structural complexity. The plasma membrane a selectively permeable barrier, encloses the cell, regulating the flow of materials. This critical structure not only protects the cell's interior but also maintains its shape and integrity. A gel-like substance called the cytoplasm fills the inner space of cell, acting as a platform for various specialized structures called organelles to carry out their essential functions. One of the most important organelles is the nucleus, typically found near the center and enclosed by its own membrane. This nucleus houses the cell's genetic material, DNA, which acts as the blueprint for everything the cell does, from growth and reproduction to its specialized tasks [5][6][7][8]. Another crucial organelle is the endoplasmic reticulum, a network of membranes that comes in two flavors: rough ER, studded with ribosomes for protein production, and smooth ER, responsible for fat metabolism and detoxification within the cell [6][7][8].

The Golgi apparatus, a network of flattened sacs, acts, modifies, sorts, and distributes proteins and lipids received from the endoplasmic reticulum, ensuring they reach their designated destinations within or outside the cell. Powering these cellular activities are the mitochondria. These double-membraned organelles generate energy in the form of ATP (adenosine triphosphate). Meanwhile, lysosomes, membrane-bound sacs filled with digestive enzymes break down waste materials, worn-out organelles, maintaining cellular hygiene and defense. Finally, ribosomes, tiny molecular machines made of RNA and protein, are responsible for protein synthesis. They translate the genetic instructions from the nucleus into functional proteins that carry out various cellular tasks [6].

The cytoskeleton, a complex network of interlinking protein filaments (microfilaments, intermediate filaments, and microtubules), provides structural integrity for the cell, maintains its shape, and facilitates essential cellular processes like movement and intracellular transport [6]. In animal cells, centrioles, barrel-shaped organelles composed of microtubules, play a crucial role in cell division. They participate in the formation of the mitotic spindle, a structure that ensures the accurate segregation of chromosomes during cell replication [6].

These cellular components function in a highly coordinated manner, each contributing specialized functionalities essential for the cell's survival, growth,

and differentiated tasks within multicellular organisms. This intricate interplay between structures and their functions empowers the cell to adapt to its environment, respond to stimuli, and fulfil its designated roles within complex biological systems [6].

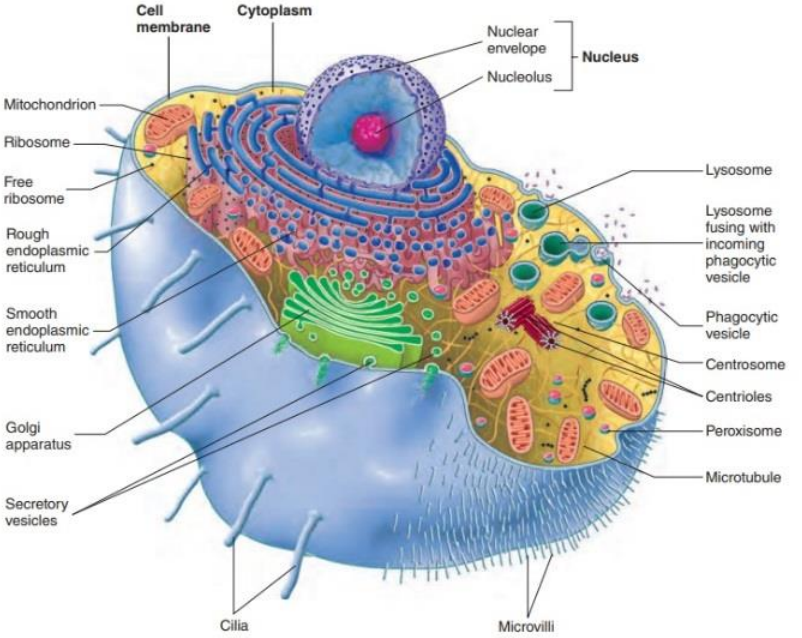

Fig. 1 Cell structure [7]

2.1 Liposome as a basic cell model

Liposomes (Fig. 2) are colloidal, vesicular structures consisting of one or more concentric bilayers formed from phospholipids [9]. Liposomes can be categorized based on various structural parameters, allowing for tailored design for specific applications [10].

Unilamellar vesicles, categorized by size as small unilamellar vesicles (SUVs; 20-100 nm), large unilamellar vesicles (LUVs; 100-250 nm), and giant unilamellar vesicles (GUVs; 1-100 μm). They offer a valuable tool for studying cell membrane mechanics due to their similar size range to cells and hence can be consist of a single phospholipid bilayer, mimicking the fundamental structure of the cell membrane [9][10].

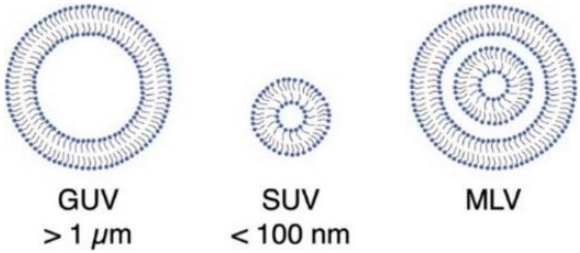

Fig. 2 Classification of liposomes [11]

2.2 Methods of giant liposome preparation

Giant unilamellar vesicles (GUVs) have been widely accepted as artificial cell models due to their comparable size range to real cells [11][12]. The first step in liposome formation is to thoroughly mix and dissolve the lipids in an organic solvent [13]. If a water-miscible organic solvent is used, liposomes can be formed by subsequently mixing the alcoholic lipid solution with an aqueous phase. The aim of this process is to obtain a clear and homogeneous lipid solution. Fig. 3 illustrates various methods of liposome production, including both conventional techniques and recently introduced in microfluidic approaches [12].

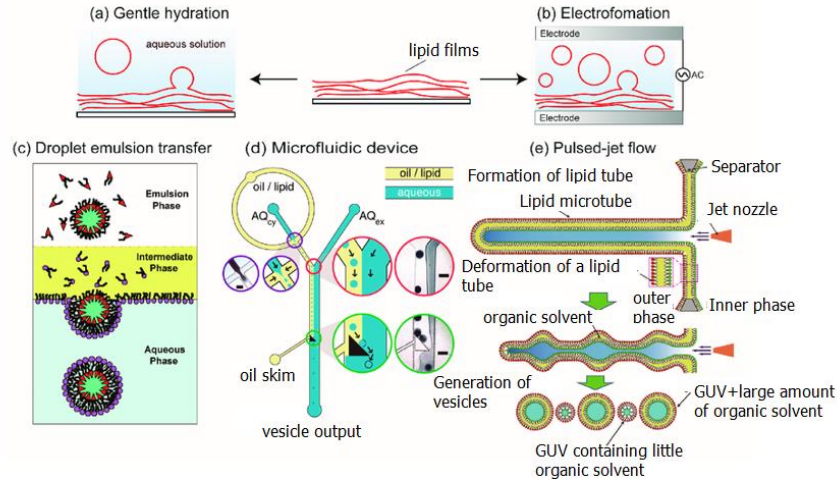

Fig. 3 Illustration of giant liposome formation (a) gentle hydration method (b) electroformation method (c) droplet emulsion transfer method (d) microfluidic devices of cell-sized lipid vesicle formations (e) pulsed-jet flow method [12]

3 Mechanical testing of cells and vesicles

Cellular mechanics play a crucial role in numerous biological processes. Deviations from these mechanical properties are often associated with various pathological conditions and diseases. Individual cells are constantly exposed to external mechanical forces that can affect their morphology and internal architecture. To gain insight into these complex relationships, researchers employ specialized tools to quantify the mechanical properties of individual cells.

3.1 Force application techniques

The force probe technique is a powerful tool in cell mechanics research. Fig. 4 provides a comprehensive overview of the various test methods used to characterize cell mechanics. It uses nanoscale probes, such as micropipettes, cantilevers, or beads, to apply or measure forces at the cell surface or even to manipulate structures within the cell. The application of force is precisely controlled by a piezo actuator, a magnetic field, or an optical trap. This technique provides valuable insights into the mechanical properties and interactions between cells and molecules. [14][15][16].

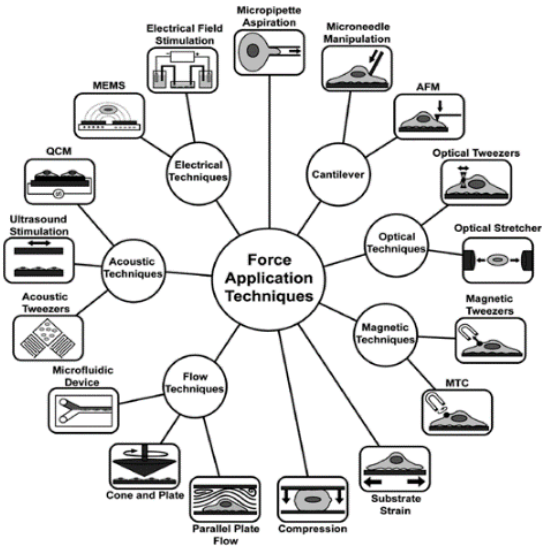

Fig. 4 Force application techniques [14]

4 Mechanical properties of cells and vesicles

The cell is composed of numerous components, each exhibiting distinct mechanical properties. Fig. 5 illustrates the various cellular components along with representative values of their mechanical properties. Additionally, the mechanical properties of cells are influenced by their surrounding environment and the external forces exerted upon them.

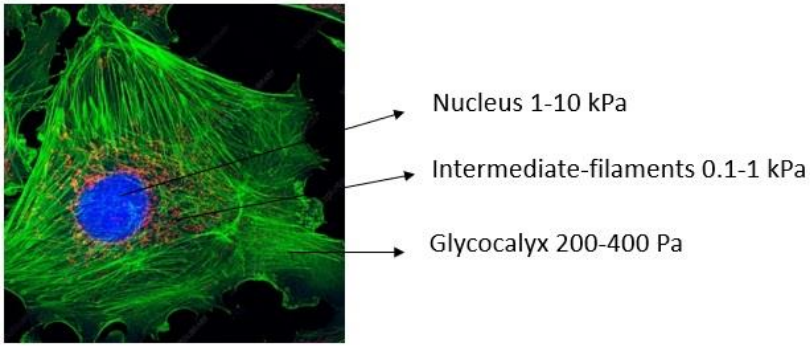

Fig. 5 Young´s modulus of the different parts of cells [21][22]

5 Aims

The mechanical characteristics of cells correlate with their condition and function, making them an inherent biophysical indicator of cell states. This includes processes like cancer cell metastasis, leukocyte activation, or advancement through the cell cycle. Cytoskeletal mechanics is a field that heavily relies on mathematical models to interpret experimental data related to forces and deformations. However, in most of the studies cells are usually described as an elastic homogeneous material. Other factors such as cytoskeleton properties, cell size, and shape, as well as the effect of environment are usually neglected. In addition to the intrinsic variations in cell properties, the method of measurement and evaluation could also affect the estimated material properties. Nowadays, there is no explicit comparison between various methods in terms of repeatability and comparability. These uncertainties are driven by large variations in mechanical properties among the cell cultures or even within the same cell measured at various positions or time intervals.

Therefore, the aim of this work is to establish a method that will provide a cell model serving as mechanical standard for evaluation of cell mechanics and use this model to verify current approaches adopted in cell mechanical testing.

The specific aim of the thesis consists of adopting microfluidic technique for liposome preparation to design and fabricate repeatable cell models with variable inner composition and tunable size. The repeatability of mechanical measurements on created cell model will be tested using various experimental approaches. Cell mechanical standard will serve as a mean for comparing estimated mechanical properties between experimental techniques and will allow to test validity of assumptions adopted in mathematical models, for example the size effect. The experimental measurements will be coupled with the development of novel theoretical models describing cell deformations based on principles of biomembrane as two-dimensional fluid crystal wrapping cell inner environment.

6 Methods

6.1 Design of microfluidic device

All computer-aided design (CAD) models of the microfluidic devices were created using SolidWorks 3D CAD design software (Dassault Systèmes SolidWorks Corporation, Waltham, MA, USA) (Fig. 6). The models incorporated variations in channel size and interchannel angles, as detailed in Tab. 1. The selection of these angles is important for the determination of the flow rate, as they exert a direct influence on the Reynolds number [41].

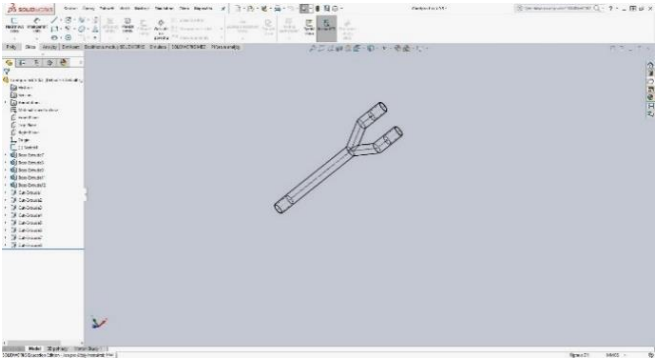

Fig. 6 CAD model of microfluidic device [41]

Tab. 1 Geometry of channels of microfluidic device

Type of manufacture	**Angle** [°]	**Size of channels Inlet / Outlet** [mm]
AM - SLA	30	0.4/0.5
		0.5, 0.75, 1/0.5
AM - SLA	60, 90	0.5/0.5
AM - PolyJet	30, 60, 90	0.5/0.5

6.2 Development of microfluidic devices by additive manufacturing

The conventional microfluidic device fabrication methods, which are primarily reliant on soft lithography, are often complex and time-consuming. Furthermore, soft lithography is inherently constrained to the fabrication of two-dimensional channel geometries. High-precision additive manufacturing techniques offer a promising alternative to conventional microfluidic device fabrication methods, enabling the creation of intricate three-dimensional structures with variable inner channel geometries. This study proposes, evaluates, and validates the application of two additive manufacturing technologies for the development of microfluidic devices [42].

6.2.1 Additive manufacturing by Stereolithography

Microfluidic devices were fabricated using a Projet® 1200 stereolithography apparatus (SLA) based on Digital Light Processing (DLP) 3D printing technology (3D Systems, Rock Hill, SC, USA). This system utilizes a beam projector to selectively cure thin layers (30 μm) of a liquid UV-curable plastic resin (VisiJet® FTX Green, 3D Systems) onto a build platform. The fabrication process involved depositing layers of the UV-curable plastic resin (VisiJet® FTX Green, 3D Systems) until the desired 3D geometry of the microfluidic channels was achieved. After printing, any uncured resin residues were removed through a washing step using an isopropyl alcohol bath. Subsequently, the microfluidic device was dried with pressurized air and subjected to a post-curing process in a UV chamber for 10 minutes. Finally, the completed device was detached from the build platform, and any supporting structures were carefully removed by hand [42].

6.2.2 Additive manufacturing by material Jetting

An alternative method for fabricating microfluidic devices was based on the use of Stratasys PolyJet technology (Stratasys Inc., Eden Prairie, MN, USA), a form of additive manufacturing based on inkjet printing. This technique involves the deposition and UV curing of photopolymer resins in a layer-by-layer manner. In this process, a Stratasys J750 printer was employed with a printing resolution of 24 × 24 × 14 microns. The microfluidic device structure was constructed using transparent Vero Clear Model® material. To maintain

the internal channel geometries throughout the printing process, a soluble support material (706 B) was employed to fill these channels. Following an initial cleaning step, the remaining support material was dissolved using a 4% sodium hydroxide and sodium silicate solution. The successful removal of the support material from the internal channels necessitated the integration of both chemical dissolution and mechanical cleaning techniques [42].

We have designed and manufactured several types of microfluidic devices, encompassing designs from simple geometries to those featuring intricate channel configurations. Details of these devices are provided in Tab. 2.

Tab. 2 Types of microfluidic devices

Used AM technology	Type of microfluidic device
Stereolitography	Y type in block
	T type in block
	Y type without block
	T type type without block
	Double three inlets channels microfluidic device
	Three inlets channels microfluidic device
Material Jetting (PolyJet)	Y type
	Three inlets channels microfluidic device

6.3 Preparation of liposomes using a microfluidic device

In this study we employed a two-stage microfluidic device utilizing the double emulsion drop method to generate liposomes. The microfluidic platform permitted the fabrication of two distinct liposome types, each optimized for a specific intended application. The first type of liposome encapsulated phosphate-buffered saline (PBS), while the second type incorporated hyaluronic acid (HA) [35] [40] [45].

6.3.1 Liposomes filled with PBS

The production of liposomes within the microfluidic device (Fig. 7 right) relies on the controlled mixing of two solutions introduced via syringes. One solution, phosphate buffer (PBS), is delivered through the two oblique channels, while the other solution, consisting of phospholipids dissolved in a mixture of isopropanol and chloroform (organic phase), is introduced through the central channel. The microfluidic design promotes lamellar flow, facilitating efficient solution interaction and liposome formation. The flow rates of the phosphate buffer solution (PBS) and the organic phase are maintained at 1 mL/h and 0.1 mL/h, respectively [23][43][51].

6.3.2 Liposomes filled with HA

Hyaluronic acid (HA)-loaded liposomes were produced using a custom designed double three inlets channels microfluidic device, (Fig. 7 left). The production process mirrors that of conventional liposomes, with key modifications to the inlet channels. HA solution is introduced through the central channel, while dissolved phospholipids in a solvent mixture (organic phase) are delivered via the first pair of opposing oblique channels intersecting the central one. The second pair of opposing oblique channels is used to feed phosphate-buffered saline (PBS). This configuration facilitates the co-localization of HA and phospholipids at the channel intersections, which enables their encapsulation within the forming liposomes [23][35][45][47][48].

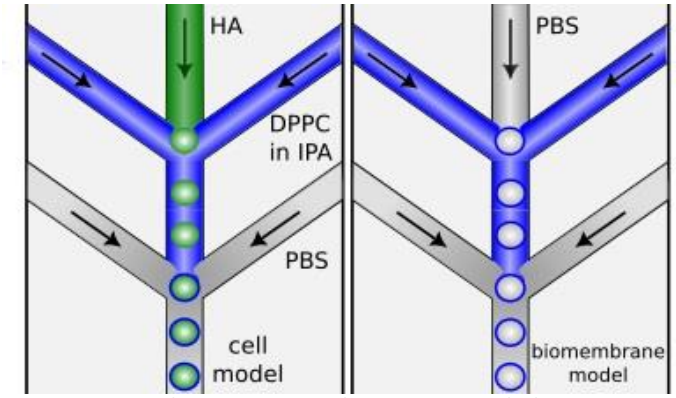

Fig. 7 Production of liposomes (right) filled with PBS (left) filled with HA [39]

6.4 Mechanical testing of liposomes

The mechanical properties of the liposomes were evaluated utilizing three distinct instruments: a NanoWizard® 3 NanoOptics Atomic Force Microscope (AFM) system (JPK Instruments, Germany), a Hysitron TI 950 TriboIndenter® nanomechanical tester (Bruker Corporation, USA), and a Bruker Hysitron BioSoft® instrument (Bruker Corporation, USA) [36][50][52].

6.4.1 Atomic force microscopy

The experiment was performed in the Laboratory of Nanotechnology at the Faculty of Biomedical Engineering, CTU, in Kladno with NanoWizard® Sense AFM System (JPK, DE). AFM system is combined with a confocal fluorescence microscope. A colloidal probe with a diameter of 5.2 μm (APPnano, CA, USA) is located at the end of the beam (spring rigidity constant of 0.0307 N/m) which deforms during indentation [36]

Force spectroscopy of the liposomes (Fig. 8) was performed with a z length of 15 μm, a relative set point of 20 nN, and the loading rate was 3.75 μm/s. The following inclusion criteria are applied: the isolated spherical shape of the liposome without collapse [24] or extensive adhesion to the surface [25], and at least two successful measurements in each liposome. Force-deformation curves were measured in the center of the liposome [36].

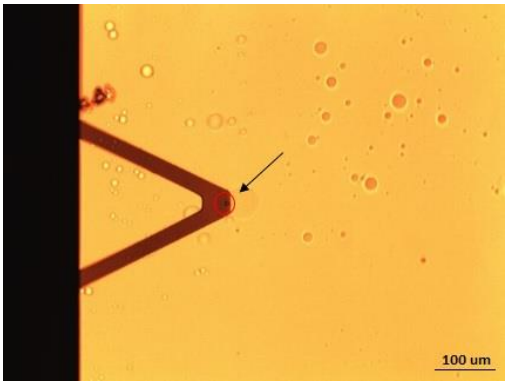

Fig. 8 AFM tip with measured liposome [36]

6.4.2 Microcompression testing using miroindenter with extended movement of the tip

Bruker's Hysitron BioSoft In-Situ Indenter was used for compression testing of liposomes. with a diamond conospherical tip with flat end with diameter 50 μm (Bruker Corp.). Displacement controlled experiment with prescribed maximum movement of the tip 100 μm in 10 second was carried out to obtain mechanical properties of whole liposome. Screenshot of the microcompression testing of liposomes is shown in Fig. 9.[49][50][52].

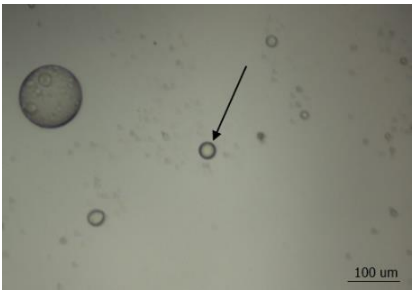

Fig. 9 Liposomes localized using a light microscope [50]

6.5 Data analysis – mathematical models

The mechanics of the cytoskeleton is a field that relies heavily on mathematical models for the interpretation of experimental data related to forces and deformations. Our models (Prescribed shape model) and (Fluid shell model) consider various factors such as stretching, bending and contact adhesion during atomic force microscopy (AFM) indentation using a spherical tip and compression testing using a flattened diamond cone tip [37][38].

6.5.1 Hertz contact model

The selection of the most appropriate Hertz model equation is dependent upon the specific geometry of the atomic force microscope (AFM) tip employed during the measurements. In this study, a spherical tip was employed. Consequently, the Young's modulus E was determined using the Hertz model for a spherical indenter, where R represents the radius of the tip [36][46].

$$F = \frac{4}{3} E^* \sqrt{R} d^{\frac{3}{2}}$$

6.5.2 Prescribed shape model

In the proposed model, the liposome is divided into two segments: the fluid membrane shell and the inner compound. The inner compound of the membrane is assumed to consist of an incompressible fluid characterized by an internal pressure denoted by p. The main assumption of the model is that liposomes undergo fully reversible adiabatic deformation, like a spring. Energy conservation implies that the external force required to deform a liposome induces deformation energy within the liposome itself. Being incompressible, the inner fluid of the liposome experiences no significant change in volume under compression or expansion and therefore cannot store energy in the form of elastic potential energy. However, the liposome membrane shell is deformable and can store strain energy. The amphiphilic nature of the lipid membrane imparts fluidity in the plane of the membrane and resistance to mechanical stress [26]. Particularly strain and bending. The stretching energy (U_S) can be expressed as follows [27][37][46].

$$U_{s=\frac{1}{2}\int K_A\,\Theta^2 d_A}$$

Here, K_A represents the area compressibility modulus [27], and Θ denotes the relative change in the segment dA induced by loading. Assuming membrane fluidity conditions equilibrium in Θ across the surface of the liposome [28] neglecting shear stresses can be simplified as follows [29][37]:

$$U_{s=\frac{1}{2}K_A(\frac{\Delta A}{A})^2 A}$$

Another contribution to the deformation energy of the membrane arises from bending. Bending energy represents the energy required to curve a membrane. A biological membrane, as a two-dimensional surface spanning a three-dimensional space, can be characterized by two principal curvatures, C_1 and C_2. The energy of biomembrane bending can be expressed using the Helfrich-Canham functional [30][37].

$$U_B = \frac{1}{2}\int K_B\,(C_1 + C_2 - C_0)^2 d_A$$

In this equation, K_B represents the bending modulus, and C_0 denotes the intrinsic curvature [31]. Contact energy refers to the excess free energy due to the existence of an interface, arising from imbalanced molecular forces [32]. It can be expressed as an energy per unit area, known as the specific surface energy γ. Contact adhesion energy (U_c) can be expressed as follows [37]:

$$U_c = \gamma A_c$$

Here, A_c represents the contact area.

If the shape of the liposome is known, we can determine the total deformation energy [37]:

$$U_{def} = U_S + U_B + U_C$$

To obtain a simple approach for calculating the total elastic deformation energy, we assume that the shape of the liposome membrane possesses azimuthal symmetry. Furthermore, we assume that the membrane is deformed by a spherical indenter of radius R_0. After deformation, the membrane has a torus-like shape with the maximum deflection in the axis of symmetry. The bilayer profile is represented by three circular arcs and a line segment representing contact with the surface (Fig. 10) [37].

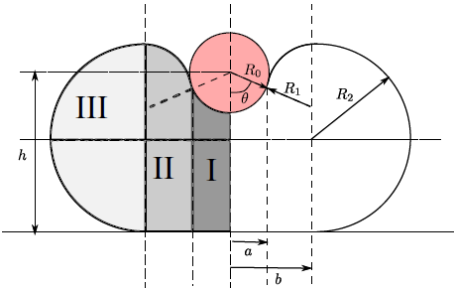

Fig. 10 Geometry of spherical AFM tip and membrane interaction [37][46]

The tip interacts with a liposome attached to the surface. The problem is axisymmetrical and individual segment of the cell membrane are described as elements of circle. The curve describing the outline of the sphere is smooth. The membrane could be divided into four segments that define four separate volumes [37].

Tab. 3 Segments of model

Segments of AFM tip and membrane interaction	Description of the segment	
Segment I	Liposome attached to AFM tip	radius equals to the radius of AFM tip, size given by angle θ
Segment II	Radius R_1	Given by angle θ
Segment III	Donut shape segment	Radius R_2
Segment IV	Liposome attached to the surface	Circle with radius b

6.5.3 Fluid shell model

The model described below is restricted to shapes with rotational symmetry. Their principal curvatures are those along the meridians (c_m) and the parallels of latitude (c_p). Let the contour of a cell be given by a function $z(x)$, the z-axis being the rotational axis. By ψ we denote the angle made by the rotational axis and the surface normal of the cell surface (Fig. 11). With this notation we find [38]:

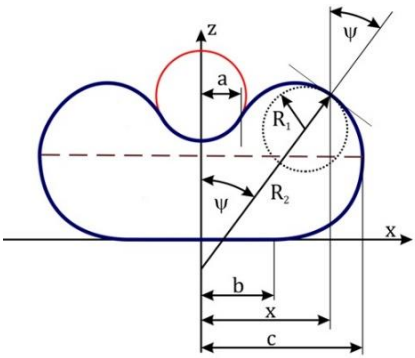

Fig. 11 Schema of the cell shape model during indentation [38]

The energy of stretching (U_S) could be expressed as [38]:

$$U_S = \int \frac{1}{2} \kappa_A \Theta^2 dA$$

where K_A is the area compressibility modulus and Θ is the relative change in segment dA induced by loading. Membrane fluidity conditions equilibrium in Θ over the surface of liposome if the shear stresses are neglected. The total area of the membrane consists of free membrane, membrane in contact with AFM tip, and the flat membrane in contact with surface. Therefore, it can be simplified into [38]:

$$U_S = \frac{1}{2} \kappa_A \left(\frac{\Delta A}{A} \right)^2 A$$

In experimental setup, the displacement of spherical tip δ is measured. The force required to induce deformation Q can be computed using the Castigliano's first theorem [38].

$$Q = \frac{\partial U_{def}}{\partial \delta}$$

6.6 Statistical analysis

Statistical analyses were performed with the R software (version 4.1.2, R Core Team, 2021). A p-value less than 0.05 was considered statistically significant. The normality of the data was tested using the Shapiro-Wilk test. The differences in materials properties between different liposome types or treatments were analyzed using one-way analysis of variance (ANOVA) followed by Tukey's post hoc test for normally distributed data and by Kruskal-Wallis test otherwise. Difference between the groups was estimated using t-test for normally distributed data and by Wilcoxon rank sum test otherwise. The linear correlation variables were assessed using linear regression (package lme4) considering repeated measurements and characterized by Pearson correlation coefficient [33].

7 Results

7.1 Additive manufacturing of microfluidic device

The production of liposomes utilised a microfluidic device that was specifically designed to mimic the basic cellular structures. This device was fabricated using additive manufacturing techniques, specifically stereolithography and PolyJet technology [41][42]. Following a thorough evaluation of both 3D printing methods, stereolithography was chosen due to its superior ability to generate smoother surface features, which are critical for optimal microfluidic device performance. Fig. 12 presents the final 3D-printed microfluidic devices employed for liposome production [42]

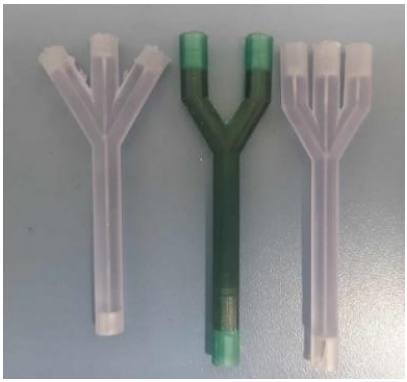

Fig. 12 The final 3D printed microfluidic devices

7.2 Hertz contact model

7.2.1 Effect of cell's size on elasticity

Hertz model was chosen as gold standard to evaluate force curves (Fig. 13) for all liposomes of nonlinear characteristics. The Hertz contact model describing elastic contact between rigid spherical indenter and an elastic half-space [36].

Linear regression (Fig. 14) was used to test whether liposome size significantly predicts Young's modulus. For both liposomes filled with PBS and HA, the effect of liposome diameter d is statistically significant and negative ($\beta = 23.44$, 95% *CI* [-28.33, - 18.56], $p < 0.001$ for the liposome filled with PBS and $\beta = -36.53$, 95% *CI* [-45.58, -27.48], $p < 0.001$ for liposomes filled with HA). The

effect of liposome diameter on Young's modulus is significantly higher for HA-filled liposomes (ANOVA p = 0.008) [36].

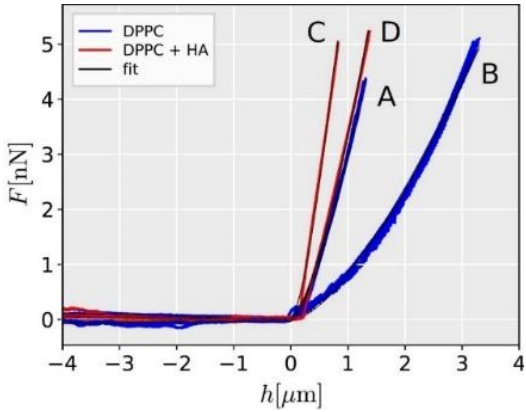

Fig. 13 Measured indentation curve for DPPC liposomes in PBS filled with (DPPC) PBS and (DPPC+HA) HA solution. Fit of indentation by Hertz contact model for hemispherical AFM tip is shown [36]

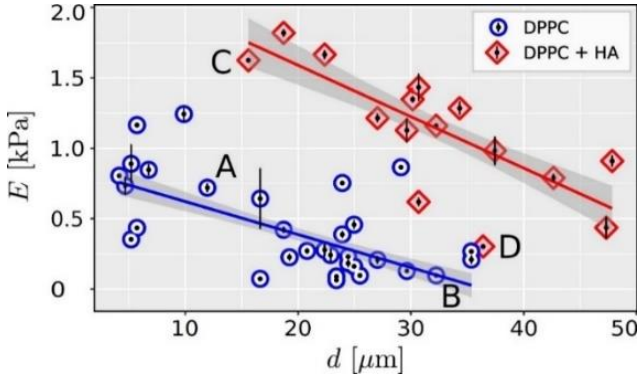

Fig. 14 Linear regression plot with 95 % confidence intervals (shaded areas) showing measured dependence between the size of DPPC liposomes and Young's modulus estimated from Hertz model measured data along with the range of measured values are shown for liposomes filled with PBS and HA solution, denoted as DPPC and DPPC+HA, respectively [36]

7.2.2 Experimental evaluation of force distribution between cytoplasm and biomembrane

Cell models with viscous cytoplasm exhibit on average higher stiffness than liquid-filled liposomes (Fig. 15 A, B)indicating an important role of cytoplasm in load transfer (Hertz model elasticity modulus 1360±271 Pa and 270±104 Pa for HA-filled and fluid-filled liposomes respectively, the difference is statistically significant t (109) = 32.47, p < 0.001). In initial contact, the load bearing capacity of both membrane and cytoplasm cell is comparable (Fig. 15 B,C). However, for deformations larger than 0.2 μm, the effect of cytoplasm prevails, and cytoplasm bears more than 80% of the overall load [39].

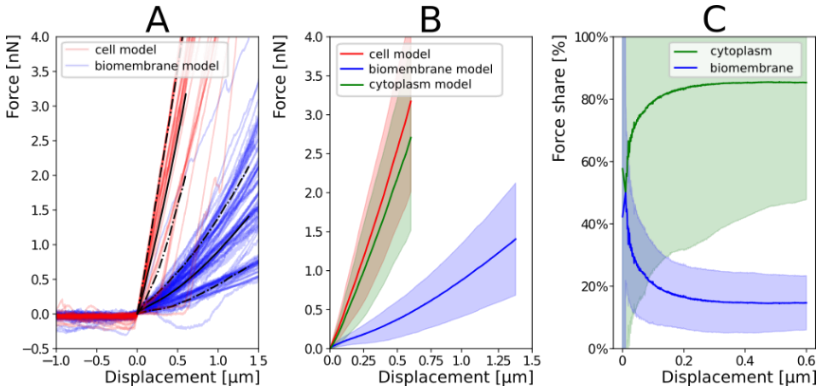

Fig. 15 (a) Force deformation curves of whole cell model (biomembrane + viscous cytoplasm) and empty liposome (biomembrane model); (b) average force curves and estimation of load transmitted through cytoplasm; (c) relative contribution of cytoplasm and biomembrane to the load bearing capacity [39]

7.2.3 Custom fitting algorithm - Hertz contact model

The Hertz model provides a good fit to the AFM data. For liposome filled with PBS (Fig. 16 left), the estimated Young´s modulus is not a function of indentation force or depth (Kruskal-Wallis rank sum test p = 0.175, chi-squared = 3.486, df = 2). The Young´s modulus evaluated at indentation force 1 nN exhibits similar variance to the one evaluated at 3 nN and 5 nN (F variance test F = 1.026, num df = 115, p = 0.892 and F = 1.262, num df = 115, p = 0.214, respectively). The difference in variance in Young´s modulus evaluated at 3 nN

and 5 nN does not significantly differs (F variance test $F = 1.230$, num $df = 115$, $p = 0.269$).

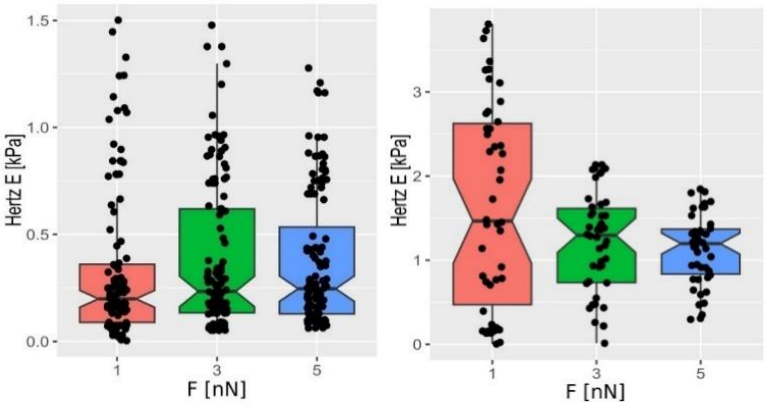

Fig. 16 Boxplot of measured Young´s modulus estimated by Hertz contact model for (left) liposomes filled with PBS and (right) liposomes filled with HA at the indentation forces 1 nN, 3 nN, 5 nN

For liposome filled with HA (Fig. 16 right), we observe decrease of estimated Young´s modulus with depth, although the observed trend is not significant (Kruskal-Wallis rank sum test $p = 0.169$, chi-squared = 3.552, $df = 2$). The Young´s modulus evaluated at indentation force 1 nN does exhibit significantly higher variance than the one evaluated at 3 nN and 5 nN (F variance test $F = 4.119$, num $df = 45$, $p < 0.001$ and $F = 8.313$, num $df = 45$, $p < 0.001$, respectively). The difference in variance in Young´s modulus evaluated at 3 nN and 5 nN is at border of statistical significance (F variance test $F = 2.018$, num $df = 45$, $p = 0.020$).

7.3 Prescribed shape model

The predicted shape of liposomes based on the developed mathematical model is visualized in Fig. 17. As the displacement of the spherical indenter increases, the deformation of the liposomes also increases. At larger deformations, the liposomes become more bulged, resulting in increased contact with both the indenter and the substrate. For displacements lower than 2 μm, the entire liposome deforms uniformly, while at higher displacements, the indenter significantly recesses into the liposome [37].

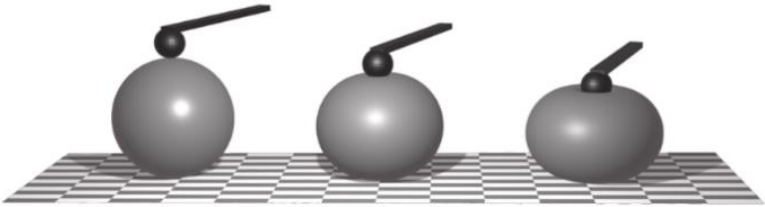

Fig. 17 Shape of liposome during mechanical testing. the displacement of the spherical indenter increases from left to right (0 µm on the left, 7.5 µm in the middle, and 15 µm on the right). The AFM spherical indenter and cantilever are schematically represented in black [37]

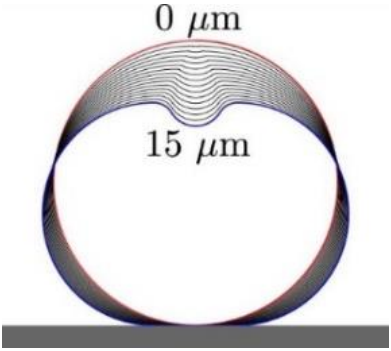

Fig. 18 Contours of liposomal shape during mechanical testing. each contour corresponds to a 1 µm increment in displacement, ranging from 0 to 15 µm [37]

Measured curves were fitted with newly defined liposome deformation model. The model is based on prescribed axisymmetric geometry and dependence between the deformation and force is estimated from the deformation energy of membrane. As the bending energy is negligible, only the stretching energy was considered within this analysis. The stiffness of the membrane in stretching is defined by the area compressibility modulus K_A.

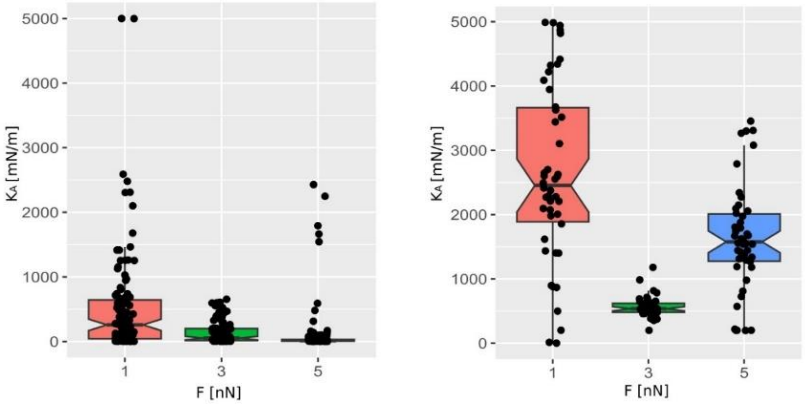

Fig. 19 Boxplot of measured area compressibility modulus estimated by prescribed shape model for (left) liposomes filled with PBS and (right) liposomes with HA at indentation forces of 1 nN, 3 nN and 5 nN

7.4 Fluid shell model

Fluid shell model is based on the Laplace equation, specifically designed for the analysis of fluid membranes. In this section, we conduct a fundamental analysis of the model's parameters and compare them to experimental data. Fig. 20 shows the change of shape in dependency on the parameter *a* which is dependent on the displacement of indentation [38].

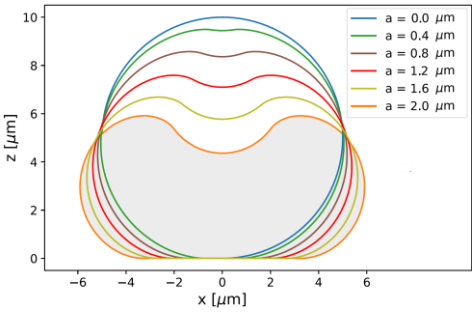

Fig. 20 Cell change shape during the indentation [38]

The dataset for nonlinear force-deformation curves was fitted with the fluid shell model. The material parameter of the model is the biomembrane area compression modulus K_A.

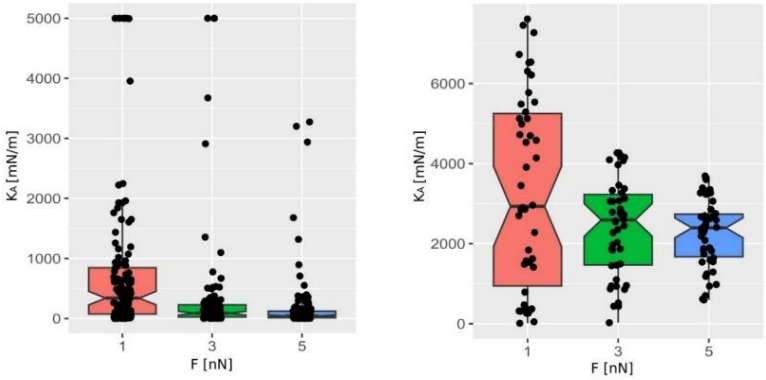

Fig. 21 Boxplot of measured area compressibility modulus estimated by fluid shell model for (left) liposomes filled with PBS and (right) liposomes filled with HA at indentation forces of 1 nN, 3 nN, and 5 nN

8 Conclusion

This study presents a two-stage microfluidic device utilizing the double emulsion drop method for the efficient and controlled production of liposomes with varying compositions. This microfluidic approach offers a cost-effective and time-saving method compared to traditional techniques. We demonstrate the versatility of this approach by generating two types of liposomes: one encapsulating phosphate-buffered saline (PBS) and another mimicking the viscous cytoplasm by incorporating hyaluronic acid (HA). These liposomes serve as artificial cell models for the investigation of their mechanical properties [34][39].

Atomic force microscopy (AFM) was employed to acquire force-deformation curves of individual liposomes [36]. Statistical analysis confirmed the high reproducibility of measurements obtained using these cell models [36][39]. To further enhance the reliability of single-cell mechanics methods, identifying potential sources of variability between individual cells is crucial. Aside from inherent physiological variations, the testing methodology and subsequent data processing can introduce technical variability. Based on the acquired measurements, it becomes evident that cell size, a factor neglected in the Hertz model's fundamental assumptions, significantly impacts the measured stiffness and estimated Young's modulus [36][39]. Therefore, comparisons between individual cells should involve cells with comparable sizes.

We further investigated the load-bearing ratio between the cytoplasm and the biomembrane. Our observations revealed a near 1:1 ratio at minimal indentation depths (less than 0.2 μm). However, this ratio progressively increases to a steady 4:1 at greater indentation depths (> 0.2 μm). These findings support the applicability of the continuum approach for analyzing cell mechanics at larger deformations. Conversely, at minimal deformations, the contribution of the cell membrane becomes significant and necessitates its inclusion in the analysis [39].

To emphasize the importance of the biomembrane, we introduce two novel models: the prescribed shape model, based on the geometrical deformation of the liposome, and the fluid shell model, which incorporates the Laplace equation for a fluid membrane [37][38]. These models acknowledge stretching as the primary deformation mode. Deviating from conventional continuum mechanics models, this innovative approach considers the entirety of the cell deformation and offers predictions regarding the contact area between the AFM tip and the substrate. Both models accurately reflect the size-dependent relationship between liposome indentation force [37][38]. However, the prescribed shape model exhibits a dependence of the constitutive parameter on indentation depth and lower repeatability [37]. We may conclude that the fluid shell model is better suited for DDPC liposomes, and the resulting material properties align with established literature values [38].

Our research demonstrates the potential of utilizing experimental models to examine key characteristics of cell mechanics. Further research is warranted to develop an experimental model that accurately represents specific living cells with intricate internal structures [37][38].

9 References

[1] FLETCHER, Daniel A.; MULLINS, R. Dyche. Cell mechanics and the cytoskeleton [online]. Nature, 2010, 463.7280: 485-492. [Accessed. 13.12.2023]. Available at: https://doi.org/10.1038/nature08908

[2] Bose, D. Six main cell functions [online]. Sciencing, 2019, [Accessed. 13.12.2023]. Available at: https://sciencing.com/six-main-cell-functions-6891800.html

[3] QUAN, Fu-Shi; KIM, Kyung Sook. Medical applications of the intrinsic mechanical properties of single cells [online]. Acta biochimica et biophysica Sinica, 2016, 48.10: 865-871. [Accessed. 13.12.2023]. Available at: https://doi.org/10.1093/abbs/gmw081

[4] DE PASCALIS, Chiara; ETIENNE-MANNEVILLE, Sandrine. Single and collective cell migration: the mechanics of adhesions [online]. Molecular biology of the cell, 2017, 28.14: 1833-1846. [Accessed. 13.12.2023]. Available at :https://doi.org/10.1091/mbc.e17-03-0134

[5] BOLSOVER, Stephen R., et al. Cell biology: a short course [online]. John Wiley & Sons, 2011, [Accessed. 13.12.2023]. Available at: http://www.bio-nica.info/Biblioteca/Bolsover2004CellBiology.pdf

[6] ALBERTS, Bruce. Molecular biology of the cell. Garland science, 2017,

[7] Cell structure [online]. BrainKart. [Accessed. 13.12.2023]. Available at: https://www.brainkart.com/article/Cell-Structure_21751/

[8] Bailey, R. Function, structure, and composition of the cell membrane [online]. ThoughtCo, 2019, [Accessed. 13.12.2023]. Available at: https://www.thoughtco.com/cell-membrane-373364

[9] PANDEY, Himanshu; RANI, Radha; AGARWAL, Vishnu. Liposome and their applications in cancer therapy [online]. Brazilian archives of biology and technology, 2016, 59. [Accessed. 13.12.2023]. Available at: https://doi.org/10.1590/1678-4324-2016150477

[10] SHASHI, Kant, et al. A complete review on: Liposomes. International research journal of pharmacy, 2012, 3.7: 10-16.

[11] LOWE, Lauren A.; LOO, Daniel WK; WANG, Anna. Methods for forming Giant Unilamellar fatty acid vesicles. Membrane Lipids: Methods and Protocols, 2022, 1-12.

[12] TOSAKA, Toshiyuki; KAMIYA, Koki. Function Investigations and Applications of Membrane Proteins on Artificial Lipid Membranes [online]. International Journal of Molecular Sciences, 2023, 24.8: 7231. [Accessed. 13.12.2023]. Available at: https://doi.org/10.3390/ijms24087231

[13] KOTOUČEK, Jan, et al. Preparation of nanoliposomes by microfluidic mixing in herring-bone channel and the role of membrane fluidity in liposomes formation [online]. Scientific reports, 2020, 10.1: 5595. [Accessed. 13.12.2023]. Available at: https://www.nature.com/articles/s41598-020-62500-2

[14] RODRIGUEZ, Marita L.; MCGARRY, Patrick J.; SNIADECKI, Nathan J. Review on cell mechanics: experimental and modeling approaches [online]. Applied Mechanics Reviews, 2013, 65.6: 060801. [Accessed. 13.12.2023]. Available at: https://doi.org/10.1115/1.4025355

[15] BACKHOLM, Matilda; BÄUMCHEN, Oliver. Micropipette force sensors for in vivo force measurements on single cells and multicellular microorganisms [online]. Nature protocols, 2019, 14.2: 594-615. [Accessed. 13.12.2023]. Available at: https://doi.org/10.1038/s41596-018-0110-x

[16] WANG, Haoqing, et al. Micropipette-based biomechanical nanotools on living cells [online]. European Biophysics Journal, 2022, 51.2: 119-133. [Accessed. 13.12.2023]. Available at: https://doi.org/10.1007/s00249-021-01587-5

[17] KONTOMARIS, S. V.; MALAMOU, A. Hertz model or Oliver & Pharr analysis? Tutorial regarding AFM nanoindentation experiments on biological samples [online]. Materials Research Express, 2020, 7.3: 033001. [Accessed. 14.12.2023]. Available at: https://iopscience.iop.org/article/10.1088/2053-1591/ab79ce/meta

[18] TIMOSHENKO, S.; GOODIER, J. N. Theory of Elasticity, McGraw Hill Inc. 1951

[19] POPOV, Valentin L., et al. Contact mechanics and friction [online]. Berlin: Springer Berlin Heidelberg, 2010, [Accessed. 14.12.2023]. Available at: https://link.springer.com/content/pdf/10.1007/978-3-662-53081-8.pdf

[20] OVERBECK, Achim, et al. Compression Testing and Modeling of Spherical Cells–Comparison of Yeast and Algae [online]. Chemical Engineering & Technology, 2017, 40.6: 1158-1164. [Accessed. 14.12.2023]. Available at: https://doi.org/10.1002/ceat.201600145

[21] YUSIFLI, Elmar, et al. Embedded Cell Count Algorithm for Cultured Tissue Characterization [online]. IFAC-PapersOnLine, 2018, 51.30: 683-687. [Accessed. 14.12.2023]. Available at: https://doi.org/10.1016/j.ifacol.2018.11.221

[22] KRIEG, Michael, et al. Atomic force microscopy-based mechanobiology [online]. Nature Reviews Physics, 2019, 1.1: 41-57. [Accessed. 14.12.2023]. Available at: https://doi.org/10.1038/s42254-018-0001-7

[23] JAHN, Andreas, et al. Microfluidic mixing and the formation of nanoscale lipid vesicles [online]. ACS nano, 2010, 4.4: 2077-2087. [Accessed. 14.12.2023]. Available at: https://doi.org/10.1021/nn901676x

[24] RUOZI, Barbara, et al. Application of atomic force microscopy to characterize liposomes as drug and gene carriers [online]. Talanta, 2007, 73.1: 12-22. [Accessed. 14.12.2023]. Available at: https://doi.org/10.1016/j.talanta.2007.03.031

[25] VORSELEN, Daan, et al. Mechanical characterization of liposomes and extracellular vesicles, a protocol [online]. Frontiers in molecular biosciences, 2020, 7: 139. [Accessed. 14.12.2023]. Available at: https://doi.org/10.3389/fmolb.2020.00139

[26] Israelachvili JN. Intermolecular and Surface Forces. Book. Elsevier, 2021, Pages 635-660. ISBN: 978-0-12-375182-9. doi.org/10.1016/C009-0-21560-1

[27] Boal, D. Mechanics of the Cell. In: Africa (Lond). Cambridge: Cambridge University Press. 1-19. 2002. ISBN: 0 521 79681 4

[28] EVANS, E. As; WAUGH, R.; MELNIK, L. Elastic area compressibility modulus of red cell membrane [online]. Biophys J. Vol. 16. 585-95. 1972. [Accessed. 14.12.2023]. Available at: https://www.cell.com/biophysj/pdf/S0006-3495(76)85713-X.pdf

[29] Evans EA, Skalak R. Mechanics and Thermodynamics of Biomembranes. CRC Press; 1978. DOI: 10.1201/9781351074339.

[30] DANIEL, Matej, et al. Clustering and separation of hydrophobic nanoparticles in lipid bilayer explained by membrane mechanics [online]. Scientific Reports, 2018, 8.1: 10810. [Accessed. 14.12.2023]. Available at: https://doi.org/10.1038/s41598-018-28965-y

[31] MARTÍNEZ-BALBUENA, L., et al. Application of the Helfrich elasticity theory to the morphology of red blood cells [online]. American Journal of Physics, 2021, 89.5: 465-476. [Accessed. 14.12.2023]. Available at: https://doi.org/10.1119/10.0003452

[32] DANIEL, Matej, et al. Modelling the role of membrane mechanics in cell adhesion on titanium oxide nanotubes [online]. Computer Methods in Biomechanics and Biomedical Engineering, 2023, 26.3: 281-290. [Accessed. 14.12.2023]. Available at: https://doi.org/10.1080/10255842.2022.2058875

[33] Bates, D., M¨achler, M., Bolker, B., & Walker, S. 2015, Fitting Linear Mixed-Effects Models Using lme4. J. Stat. Softw., 67, 1–48.

[34] MARCOTTI, Stefania; REILLY, Gwendolen C.; LACROIX, Damien. Effect of cell sample size in atomic force microscopy nanoindentation [online]. Journal of the Mechanical Behavior of Biomedical Materials, 2019, 94: 259-266. [Accessed. 14.12.2023]. Available at: https://doi.org/10.1016/j.jmbbm.2019.03.018.

10 List of publications related to the dissertation thesis

Articles

[35] HILŠER, P., MENDOVÁ, K., et al. A new insight into more effective viscosupplementation based on the synergy of hyaluronic acid and phospholipids for cartilage friction reduction. Biotribology. 2021, 25(2352-5738), ISSN 2352-5738. DOI 10.1016/j.biotri.2021.100166

[36] MENDOVÁ, K., et al. Rethinking Hertz Model Interpretation for Cell Mechanics Using AFM. International Journal of Molecular Sciences. Manucsript number: ijms-3036525, Under Review., doi:10.20944/preprints202405.1183.v1

[37] MENDOVÁ, K., M. DANIEL, and M. OTÁHAL. Nonlinear cell deformation model. Journal of Mechanical Engineering. 2023 ISSN 2450-5471. DOI 10.2478/scjme-2023-0026

[38] M. OTÁHAL., MENDOVÁ, K, and M. DANIEL. AFM cell indentation: fluid shell model. In: Proceedings of 2023 EHealth and Bioengineering Conference (EHB). IEEE International Conference on e-Health and Bioengineering EHB 2023 - 11-th edition, Bucuresti, 2023-11-09/2023-11-10. Iasi: Gr. T. Popa University of Medicine and Pharmacy, 2023. ISBN 979-8-3503-2887-5

[39] MENDOVÁ, K., et al. Experimental evaluation of force distribution between cytoplasm and biomembrane. Journal of the Mechanical Behavior of Biomedical Materials. Manucsript number: JMBBM-D-24-00956, Under Review.

Book chapters

[40] MENDOVÁ, K., M. DANIEL, and J. ŘEZNÍČKOVÁ. Interactions between biomembrane embedded nanoparticles mediated by lipid bilayer [online]. In: Kordogiannis, G., ed. Advances in Biomembranes and Lipid Self-Assembly. Elsevier Inc, 2021. p. 1-16. ISSN 2451-9634. [Accessed. 14.12.2023]. Available at: https://doi.org/10.1016/bs.abl.2023.09.001

Conference contributions

[41] MENDOVÁ, K. and P. RŮŽIČKA. Rapid development of microfluidic device using additive manufacturing. In: MORAVEC, J., ed. Studentská tvůrčí činnost 2019. Konference studentské tvůrčí činnosti 2019, Technická 4, Praha 6, 2019-04-09. Praha: České vysoké učení technické v Praze, Fakulta strojní, 2019. p. 15. ISBN 978- 80-01-06564-8. Available from: http://stc.fs.cvut.cz/docs/program_2019_a.pdf

[42] MENDOVÁ, K., M. DANIEL, and P. RŮŽIČKA. Development microfluidic device using additive manufacturing. In: VONDROVÁ, J. and Z. PADOVEC, eds. 24th Workshop of applied mechanics - book of papers. 24th Workshop of Applied Mechanics, ČVUT FS, 2018-06-08. Praha: CTU FME. Division of strength and elasticity, 2018. ISBN 978-80-01-06453-5.

[43] MENDOVÁ, K., K. ELERŠIČ FILIPIČ, and M. DANIEL. Protocol of production of cell sized liposomes using microfluidic device and the effect of plasma treated glass on liposomes fixation. In: PELIKÁN, J., ed. 27th Workshop of Applied Mechanics - Proceedings. Praha: České vysoké učení technické v Praze, Fakulta strojní, 2019. ISBN 978-80-01-06680-5.

[44] MENDOVÁ, K., et al. Experimental evaluation of liposomes biomechanics. In: KUBÁŠOVÁ, K. and Z. PADOVEC, eds. 29th Workshop of applied mechanics book of papers. 29th Workshop of Applied Mechanics, Praha, 2021-11-05. Praha: CTU FME. Department of Mechanics, Biomechanics and Mechatronics, 2021. ISBN 978-80-01-06909-7.

[45] MENDOVÁ, K., et al. 2v1: Lipozóm ako model bunky/nosič liečiv? In: KUBÁŠOVÁ, K., et al., eds. Human Biomechanics 2023 – Sborník. Human Biomechanics 2023, Doksy, Máchovo jezero, 2023-06-26/2023-06-28. Praha: České vysoké učení technické v Praze, Fakulta strojní, 2023. p. 7. ISBN 978-80-01-07179-3.

[46] MENDOVÁ, K., et al. Experimental and analytical evaluation of the biomechanics of liposomes. In: 24th International Scientific Conference Applied mechanics 2023 Book of abstracts. 24th International conference applied mechanics, Piešťany, 2023-04-19/2023-04-21. Bratislava: Strojnícka fakulta STU v Bratislave, 2023. p. 79-80. ISBN 978-80-227-5294-7.

[47] MENDOVÁ, K., et al. Znižujú lipozómy súčiniteľ trenia v chrupavke? In: SUCHÝ, T., et al., eds. Biomateriály a jejich povrchy XIV. Herbertov, Horní mlýn, 2021-09-14/2021-09-17. Praha: Czech Technical University in Prague, 2021. p. 9-92. 1. ISBN 978-80-01-06872-4.

[48] MENDOVÁ, K., M. DANIEL, and M. VRBKA. Vplyv lipozómov na súčiniteľ trenia v synoviálnych kĺboch. In: SUCHÝ, T., et al., eds. Biomateriály a jejich povrchy XIII. Biomateriály a jejich povrchy XIII, Herbertov, Horní mlýn, 2020-09-15/2020-09-18. Praha: Czech Technical University in Prague, 2020. ISBN 978-80-01-06754-3.

[49] MENDOVÁ, K., J. ŠEPITKA, and M. DANIEL. Mechanical properties of phospholipid layers. In: PADOVEC, Z. and J. VONDROVÁ, eds. 26th Workshop of Applied Mechanics. Praha, 2019-06-21. Praha: ČVUT v Praze, Fakulta strojní, Ústav mechaniky, biomechaniky a mechatroniky, 2019. ISBN 978-80-01-06604-1.

[50] MENDOVÁ, K. and M. DANIEL. Principles of mechanical testing of cells. In: PELIKÁN, J., ed. 23rd Workshop of Applied Mechanics - Proceedings. 23rd Workshop of Applied Mechanics, Praha, 2017-12-15. Praha: České vysoké učení technické v Praze, Fakulta strojní, 2017. p. 20-21. ISBN 978-80-01-06372-9.

[51] MENDOVÁ, K. and M. DANIEL. Tvorba lipozómov mikrofluidným zariadením. In: SUCHÝ, T., et al., eds. Biomateriály a jejich povrchy X. Praha: Czech Technical University in Prague, 2017. p. 50-51. ISBN 978-80-01-06195-4.

[52] MENDOVÁ, K., DANIEL M., ŠEPITKA J., AND OTÁHAL M. Mechanické vlastnosti buněk. In: XIV. mezinárodní konference Bioimplantologie. Praha: Národní knihovna ČR, 2023. ISBN 978-80-11-03134-3.